

# dsRNA Induced IFN $\beta$ -MMP13 Axis Drives Corneal Wound Healing

Xihong Lan, Wang Zhang, Jin Zhu, Huaxing Huang, Kunlun Mo, Huizhen Guo, Liqiong Zhu, Jiafeng Liu, Mingsen Li, Li Wang, Chunqiao Liu, Jianping Ji, and Hong Ouyang

State Key Laboratory of Ophthalmology, Zhongshan Ophthalmic Center, Sun Yat-sen University, Guangzhou, China

Correspondence: Hong Ouyang, State Key Laboratory of Ophthalmology, Zhongshan Ophthalmic Center, Sun Yat-sen University, Guangzhou 510060, China; [ouyhong3@mail.sysu.edu.cn](mailto:ouyhong3@mail.sysu.edu.cn).

XL and WZ contributed equally to this work.

**Received:** November 10, 2021

**Accepted:** January 11, 2022

**Published:** February 7, 2022

Citation: Lan X, Zhang W, Zhu J, et al. dsRNA induced IFN $\beta$ -MMP13 axis drives corneal wound healing. *Invest Ophthalmol Vis Sci.* 2022;63(2):14. <https://doi.org/10.1167/iovs.63.2.14>

**PURPOSE.** Cornea, the outermost transparent layer of the eye, is the first line of defense against external threats. Following injury, the wound healing response is crucial to corneal repair and regeneration, yet its underlying mechanism is poorly understood. Our study was designed to investigate the role of dsRNA and its regulatory network in corneal wound healing.

**METHODS.** A corneal wound healing model was established via the surgical removal of half of the corneal surface and adjoining limbus. RNase III was then used to clarify the role of dsRNA in corneal wound closure and RNA-seq was performed to investigate the mechanism of dsRNA in the healing process. Related gene expression was assessed using immunofluorescence staining, qPCR, and Western blot. Flow cytometry and scratch assay were used to analyze the proliferation and migration of limbal stem/progenitor cells (LSCs) in vitro and functional analysis of the target genes was completed using the corneal wound healing model.

**RESULTS.** Corneal wound healing was delayed and impaired when the dsRNAs were removed or damaged following RNase III digestion. The dsRNAs released following corneal damage activate type I interferon (IFN-I) signaling, primarily IFN $\beta$ , via the corneal epithelium and neutralizing IFN $\beta$  or blocking IFN-I signaling delays corneal wound closure. Moreover, our data identified MMP13 as a downstream effector of IFN $\beta$  where its expression promotes LSC proliferation and enhances corneal epithelial reconstruction in vivo.

**CONCLUSIONS.** The dsRNA induced IFN $\beta$ -MMP13 axis plays a key role in corneal wound healing.

**Keywords:** corneal injury, dsRNA, type I interferon, wound healing

The corneal surface and tear film act as the outermost barrier of the eye working to defend against damage and pathogens.<sup>1,2</sup> The continuous self-renewal of the corneal epithelium is sustained by limbal stem/progenitor cells (LSCs), located in the basal part of the limbal epithelium in the peripheral cornea.<sup>3,4</sup> Upon injury, the activated LSCs proliferate, differentiate, and migrate toward the central cornea to restore the epithelial layers.<sup>5</sup> Although the cornea acts as a mucosal surface with similar functional properties to those of the skin, and the mucus membranes of the respiratory tract and gut,<sup>6</sup> it should be noted that only the cornea needs to account for optical properties.<sup>7</sup> Thus, a successful wound response must allow for rapid repair without jeopardizing corneal clarity.

Corneal wound healing is a complex process involving programmed cell death, proliferation, migration, and extracellular matrix remodeling.<sup>8</sup> Epidermal growth factor (EGF) signaling in wounded corneas has been shown to stimulate corneal wound healing by initiating cell migration and proliferation.<sup>9-11</sup> Insulin-like growth factor (IGF)-1 expressed by corneal keratocytes and epithelial cells also plays important roles in energy metabolism, growth, cell

migration, and proliferation, and can synergistically enhance corneal wound closure when induced in the presence of substance P.<sup>12</sup> Inflammatory cytokines, such as IL-6 and IL-10, secreted by immune or epithelial cells, enhance cell migration and accelerate corneal wound healing.<sup>13</sup> However, the mechanisms underlying corneal regeneration following injury remain poorly understood.

Tissue injury results in cell necrosis and apoptosis, releasing damage-associated molecular patterns (DAMPs), including dsRNA, which functions as a cell death signal in the innate immune system.<sup>14</sup> The release of dsRNA from damaged cells has been shown to be involved in the initiation of the inflammatory response, which is crucial for normal wound repair.<sup>15,16</sup> It has been reported that dsRNA could activate Toll like receptor 3 (TLR3), which has been extensively linked to tissue regeneration process.<sup>17,18</sup> Several parallel systems have been hypothesized to respond to dsRNA induced regulation but very few have been evaluated, including corneal wound healing.

In this study, we demonstrate that the dsRNA acts as a key trigger for corneal wound healing through its induction of IFN $\beta$ . MMP13 exerts as a downstream effector of IFN $\beta$ ,

which is involved in epithelial proliferation and enhanced injury repair.

## MATERIALS AND METHODS

### Animal Model and Treatments

All animal experiments were approved by the Animal Ethics Committee at Zhongshan Ophthalmic Center and were conducted following the guidelines established by the Association for Research in Vision and Ophthalmology Statement on the Use of Animals in Ophthalmic and Vision Research.

C57BL/6 mice (4–8 weeks old) were anesthetized using sodium pentobarbital (50 mg/kg). For corneal injury model, Algerbrush II corneal rust ring remover (Alger Co., Lago Vista, TX, USA) was used to scrape half of the corneal surface and adjoining limbus. To ensure consistency of the injury depth between groups, all mice received an optical coherence tomography (OCT) scan to evaluate the thickness of the corneas before and after surgery. Vertical and horizontal lines were measured and the minimal and the maximal depth of the pathology were recorded. For dsRNA digestion, RNase III (0.6 U/ $\mu$ L (New England Biolabs, M0245S) was applied to the right eyes of the mice by subconjunctival injection (5  $\mu$ L) twice per day (Supplementary Fig. S1C) and eye drops to the wounded ocular surface 4 times per day for 3 days. Other chemicals and proteins 0.4  $\mu$ g/ $\mu$ L IFN $\beta$  antibody (ThermoFisher, PA5-20390); 0.8  $\mu$ M ruxolitinib (MedChemExpress, HY-50856); 0.3  $\mu$ g/ $\mu$ L MMP13 antibody (Proteintech, 18165-1-AP); 3 ng/ $\mu$ L recombinant mouse MMP13 (rMMP13; MyBioSource, MBS960550); and PBS and IgG (EMD Millipore, 12-371, as control) were applied to the right eyes of the mice by subconjunctival injection (5  $\mu$ L) twice per day for 3 days. To evaluate epithelial defects in wounded mice, sodium fluorescein staining areas were analyzed by software ImageJ (National Institutes of Health, Bethesda, MD, USA).

### Culture of LSCs

LSCs were cultured from limbal tissue of human donor eyes with the approval of the Ethics Committee of Zhongshan Ophthalmic Center. The culture medium of LSCs was prepared as described previously.<sup>1</sup> Briefly, limbal tissues were cut into small pieces and incubated with 0.2% collagenase IV (Gibco) solution at 37°C for 2 hours and 0.25% trypsin-EDTA (Gibco) for 15 minutes. Cells were cultivated in Collagen I-coated dishes. 400 ng/mL recombinant human IFN $\beta$  (Abbkine, PRP100183) was applied to evaluate the interferon stimulated gene expression. PBS was used as control.

### Western Blot Analysis

LSCs were washed by PBS two times and then lysed by RIPA Lysis Buffer with protease inhibitor. Mice corneas were lysed by Minute Total Protein Extraction Kit (Invent Biotechnologies, SD001) containing 1% protease inhibitor cocktail (Sigma-Aldrich, P8340). Equal amounts of protein were measured by bicinchoninic acid protein assay kit (Millipore, USA), electrophoresed on SDS-PAGE (Bio-Rad, 4561094), and transferred to a polyvinylidene difluoride (PVDF) membrane. Then, PVDF membranes were blocked with 5% bovine serum albumin (BSA) in TBS containing 0.1% Tween-20 (TBST) and incubated with primary antibodies overnight at 4°C. After incubation, the membranes

were washed with TBST and incubated with secondary antibodies conjugated by HRP. The HRP signal was visualized using the ECL kit by Bio-Rad (Bio-Rad Laboratories, USA) and analyzed by Image J software. Antibodies were listed in Supplementary Table S1.

### Hematoxylin and Eosin and Immunofluorescence Staining

Tissue samples were fixed with 10% neutral buffered formalin (NBF). After dehydration and paraffin embedding, tissues were sectioned to a thickness of 5  $\mu$ m. The tissue sections were stained with hematoxylin and eosin after de-paraffinization. LSCs were fixed with 4% paraformaldehyde overnight at 4°C. For immunofluorescence staining, tissue sections or cell samples were permeabilized and blocked using 0.3% Triton X-100 and 5% BSA for 1 hour, followed by primary antibodies incubation overnight at 4°C. After washes, sections and cells were incubated with secondary antibodies for 1 hour at room temperature. Cell nuclei was stained with DAPI (4',6-diamidino-2-phenylindole). Immunofluorescence images were captured by ZEISS LSM 800 microscope. Antibodies are listed in Supplementary Table S2.

### EdU Assay

C57BL/6 mice were injected with 50 mg/kg EdU (Beyotime Biotechnology, C0071S) following corneal injury and were euthanized 24 hours later. The eyeballs were fixed with 10% NBS. Tissue sections were incubated with Click Additive Solution for 30 minutes after dewaxing, and nuclei was stained with DAPI.

### RNA Isolation and qPCR

Total RNAs were extracted using RNeasy Mini Kit and RNeasy Protect Mini Kit (Qiagen, 74704 and 74124) and transcribed into cDNA using PrimeScript RT Master Mix (TaKaRa, HRR036A). The qPCR was performed using SYBR Green Supermix Kit (Bio-Rad, 1708880) on QuantStudio 7 Flex system (Life Technologies, USA). All samples were performed in triplicates and normalized by glyceraldehyde 3-phosphate dehydrogenase (GAPDH) levels. Primers are listed in Supplementary Table S3.

### Scratch Assay and Cell Proliferation Assay

Scratch wounds were made by 200  $\mu$ L pipette when LSCs reached 100% confluency. The recombinant human MMP13 (rhMMP13; R&D Systems, 511-MM-010) were added to the culture medium with a concentration of 1  $\mu$ g/mL. PBS was used as control. Scratch open area were photographed and analyzed by ImageJ software. For cell proliferation assay, LSCs were stained by 2.5  $\mu$ M CFSE (5,6-carboxyfluorescein diacetate succinimidyl ester). For the starting point (original fluorescence intensity), CFSE labeled LSCs were immediately fixed and stored at 4°C. The proliferation ratios were determined by flow cytometry (BD LSRFortessa cell analyzer, USA).

## RNA-Seq Data Processing

Total RNAs were extracted using RNeasy Mini Kit. RNA sequencing libraries were generated by TruSeq Stranded mRNA Library Prep kit (Illumina, 20020594) and sequenced using paired-end (2 × 125 bp) sequencing method on HiSeq Xten platform (Annoroad Gene Technology Co. Ltd.). Trimmed reads were aligned to mouse GRCm38 reference genome with STAR software (version 2.6.1a) 64 to calculate read counts of each gene. TPM values were calculated using RSEM (version v1.3.0). Differential gene expression from two biological replicates was analyzed using DESeq2 (version 1.20.0). Gene ontology (GO) biological process analysis was conducted using clusterprofiler R package (version 3.6.1, *P* value threshold 0.05, *q*-value threshold 0.05). Genes were annotated as interferon stimulated genes according to database Interferome version 2.0 (<http://interferome.its.monash.edu.au/interferome/>). All RNA sequencing data are available through Gene Expression Omnibus accession number: GSE191228.

## Statistical Analysis

All data were presented as the mean  $\pm$  standard error (SE). GraphPad software (GraphPad Software, USA) was used to perform statistical analyses. The Student's *t*-test was used to compare differences between groups. Comparisons among three or more groups were analyzed by 1-way or 2-way ANOVA followed by Bonferroni's post hoc test. \**P* value < 0.05 was regarded as a significant difference.

## RESULTS

### dsRNA is Critical to Corneal Wound Healing

We established a corneal injury model to evaluate the role of dsRNA in corneal wound healing, in which half of the limbus, corneal epithelium, and part of the stroma were surgically removed. Corneal thickness was determined using OCT which validated that all animals received a similar injury to the corneal lamella ( $29.7 \pm 1.2 \mu\text{m}$ ; Supplementary Figs. S1A, S1B). Slit-lamp microscopy and sodium fluorescein staining showed that the unwounded cornea was transparent and had no epithelial defects, whereas the half of the corneal surface was defective in wounded cornea after injury (Fig. 1A).

RNase III, the dsRNA-specific endonuclease, was applied to the wounded cornea by sub-conjunctiva injection and eye drops to digest dsRNA (see Supplementary Fig. S1C). As expected, immunostaining showed that dsRNA induced by wounding could be partially removed by RNase III treatment (see Supplementary Fig. S1D). Surprisingly, a significant delay of wound closure was observed from day 2 (d2) in RNase III-treated mice compared to the control (see Fig. 1A). Evaluation of the epithelial defect at d3 revealed that the cornea was almost healed in the control group ( $6.6\% \pm 0.4\%$  defect), whereas there was still a significant defect in the treated mice ( $30.9\% \pm 2.7\%$ ; see Fig. 1B). Meanwhile, the unwounded corneas exhibited no epithelial defects upon treatment with RNase III (see Supplementary Fig. S1E). We also observed a significant reduction in Ki67- and EdU (5-ethynyl-2-deoxyuridine)-positive cells in the corneal epithelium of RNase III-treated mice at d1, indicating a decline in the proliferative activity in the wounded cornea when dsRNA was degraded (see Figs. 1C, 1D, Supplementary

Fig. S2A). Taken together these data demonstrate that dsRNA is involved in corneal wound healing.

By d7, all of the corneal wounds were completely healed (see Figs. 1A, 1B). P63 was only expressed in the epithelial basal layer of the unwounded mice, but was distributed in each epithelial layer in both the control and RNase III-treated mice, whereas corneal specific keratin 12 (KRT12) was positively expressed across all three groups (see Fig. 1E). In addition, Keratin 6 (KRT6), the wound-response marker for the epithelium, was highly expressed in wounded corneas at d1 (see Supplementary Fig. S2B), but could not be detected when the wound was closed at d7 (see Fig. 1E). Notably, although the RNase III-treated corneal wounds were eventually repaired, fewer layers of corneal epithelium when compared to both the unwounded and control mice at d7 (see Fig. 1E). Moreover, the disarranged appearance in the stroma of RNase III-treated corneas was accompanied by opacification with positive staining of fibrosis related protein,  $\alpha$ -SMA (see Figs. 1A, 1E, Supplementary Fig. S1F). Taken together, these data suggest that interfering with the natural release of dsRNA during the wound healing process could lead to impaired corneal regeneration.

### dsRNA Activates Type I Interferon Signaling in Wounded Corneas

Given the fact that RNase III treatment delayed the closure of corneal wounds, we then went on to explore the potential mechanism responsible for dsRNA mediated wound healing using RNA sequencing. Comparison of the gene expression profiles of the wounded and unwounded corneas allowed us to identify 2681 differentially expressed transcripts in these tissues, with these transcripts clustered into three main expression patterns according to variations in their TPM values (Fig. 2A). Transcripts in group I were downregulated in wounded corneas when compared to unwounded ones (Fig. 2A) and gene ontology (GO) analysis showed that the genes preferentially expressed in group I are linked to development and differentiation pathways, such as synapse organization, cell junction assembly, and eye development. These biological events might contribute to the homeostasis of quiescent cornea. Transcripts in group II were upregulated in wounded corneas compared to unwounded corneas regardless of RNase III treatment and these genes were linked to several immunological processes, including positive regulation of response to external stimuli, cytokine production, and external stimulus-mediated signaling pathways (see Fig. 2B).

Interestingly, transcripts in group III were upregulated in wounded corneas, but attenuated in the RNase III treated samples. The genes in this group were influenced by the reduction of dsRNA and were enriched for epithelial cell proliferation, leukocyte migration, and response to wounding like those of group II, but were also specifically enriched in response to type I interferon (see Fig. 2B). Gene set enrichment analysis (GSEA) confirmed that GO term "response to type I interferon" was enriched in the control group relative to the unwounded group (see Fig. 2C) but repressed in wounded corneas treated with RNase III (see Fig. 2D). Moreover, the type I interferon responsive genes upregulated in wounded corneas, including *Isg15*, *Bst2*, *Mx1*, *Mx2*, and *Ifit1*, were significantly downregulated when evaluated in treated samples (see Fig. 2E). These results provide compelling evidence that dsRNA-activated



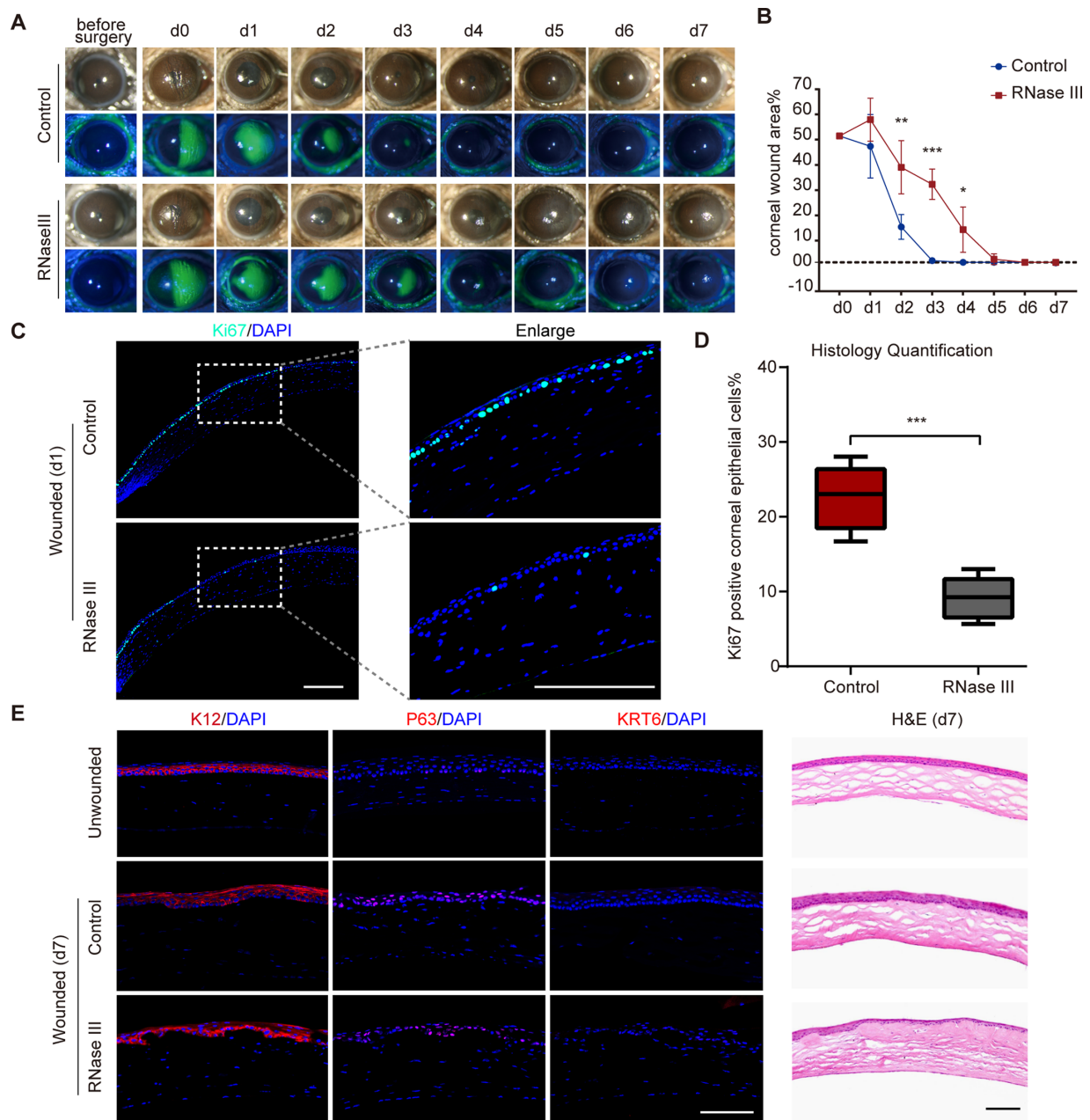


**FIGURE 1. RNase III delays corneal wound healing.** (A) Representative images of the epithelial defect in wounded corneas of control and RNase III treated group (for each treatment: *upper panel*, white light micrograph; *lower panel*, fluorescein staining of corneal surface). (B) Quantification of re-epithelialization in control and RNase III treated group. Epithelial defect is presented as the percentage of the original wound size (Students *t*-test,  $n = 5$ ). The *black asterisk* indicates a significant difference among groups ( $*P < 0.05$ ,  $**P < 0.01$ ,  $***P < 0.001$ ). (C) Representative immunofluorescence staining of Ki67 in wounded corneas (d1 post-injury). Scale bars, 200  $\mu\text{m}$ . (D) Quantifications of Ki67 positive cells from independent samples (Students *t*-test,  $n = 5$ ,  $P < 0.001$ ). (E) Representative immunofluorescence staining (*left panel*) of K12, P63, and KRT6, and H&E staining (*right panel*) in unwounded and wounded corneas at d7 post-injury. Scale bars, 100  $\mu\text{m}$ .

type I interferon signaling is involved in corneal wound healing.

### IFN $\beta$ Mediated Corneal Wound Healing

Quantitative evaluations indicated that IFN $\beta$  was significantly increased in wounded corneas and significantly decreased in RNase III-treated mice, whereas IFN $\alpha$  expression was barely detectable (Fig. 3A). Positive staining of IFN $\beta$  and KRT6 was also observed in the wounded corneal

epithelium, but not in unwounded corneas (see Fig. 3B). Thus, IFN $\beta$  is the major type I IFN in corneal epithelium wound healing, and that its induction is attenuated by the reduction of dsRNA. We then used IFN $\beta$  antibody and ruxolitinib, a JAK inhibitor known to specifically inhibit IFN $\beta$  signaling, to examine the effect of IFN signaling on corneal wound healing. An isotype-matched non-immune IgG antibody was used as a control. As expected, we noticed a marked delay in wound closure in injured corneas following 2 days of treatment with IFN $\beta$  antibody (see Figs. 3C, 3D). By



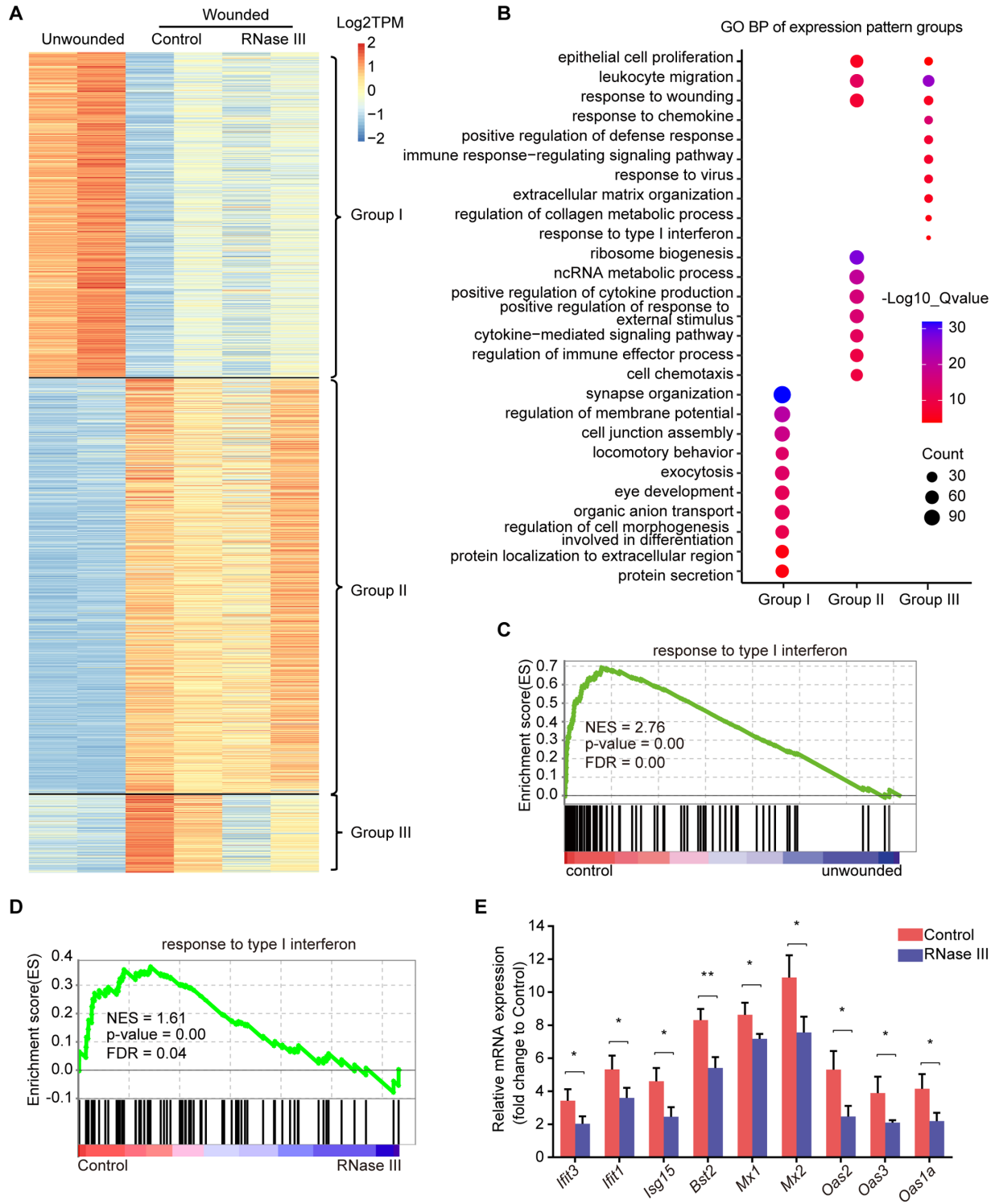


**FIGURE 2. Transcriptional profiling of corneal wounds.** (A) Heatmap of differentially regulated transcripts in mice corneas of unwounded group, wounded (control and RNase III treated group) at d1 post-injury. The candidate genes are mainly divided into three groups. (B) GO biological process (BP) analysis of genes of three groups. (C) GSEA of response to type I interferon genes that are expressed higher in wounded (control) cornea than in unwounded cornea at d1 post-injury. (D) GSEA of response to type I interferon genes that are expressed higher in wounded (control) cornea than in wounded cornea treated with RNase III (RNase III) at d1 post-injury. (E) The qPCR analysis of ISGs expression in wounded cornea treated with or without RNase III at d1 post-injury (Students *t*-test, *n* = 3). Data are represented as mean  $\pm$  SE (\**P* < 0.05, \*\**P* < 0.01).

d5, antibody-neutralized wounds were still not completely closed (1.1%  $\pm$  0.7%) and similar results were also found

in corneas treated with ruxolitinib at d3 (see Figs. 3C, 3D). Consistently, Ki67 staining and EdU assay revealed a notable

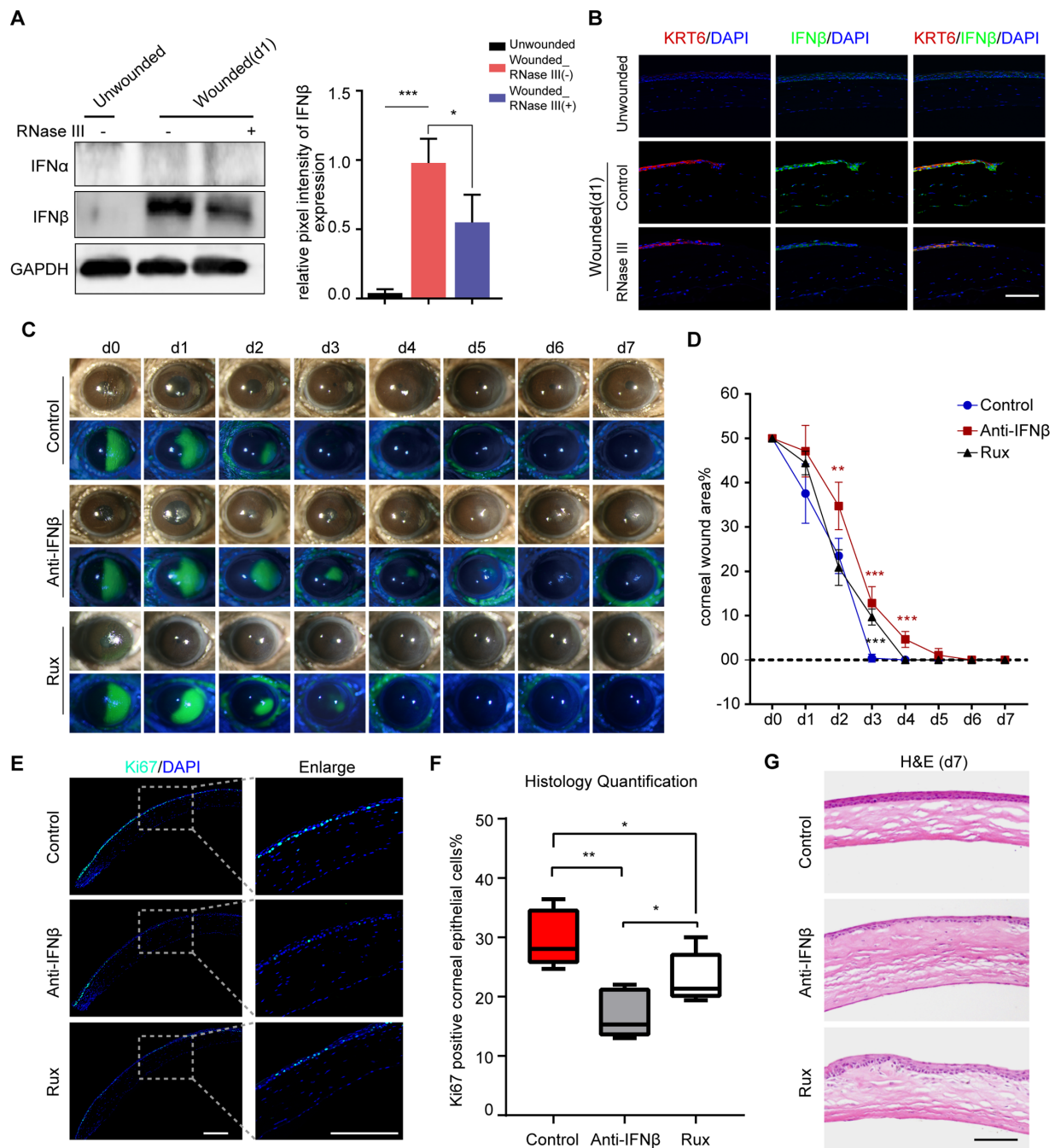


**FIGURE 3. IFN $\beta$  mediates corneal wound healing.** (A) Western blot analysis of IFN $\alpha$  and IFN $\beta$  proteins in unwounded cornea and wounded cornea at d1 treated with or without RNase III ( $n = 3$ ). Expression of IFN $\beta$  relative to GAPDH for each group was determined (Students  $t$ -test,  $n = 3$ ,  $*P < 0.05$ ,  $***P < 0.001$ ). (B) Representative immunofluorescence staining of IFN $\beta$  and KRT6 in mice corneas of each group. Scale bar, 100  $\mu$ m. (C) Representative images of the epithelial defect in wounded corneas of control, IFN $\beta$  antibody, and ruxolitinib (Rux) treatment (for each treatment: *upper panel*, white light micrograph; *lower panel*, fluorescein staining of corneal surface). (D) Quantification of re-epithelialization in control, IFN $\beta$  antibody and ruxolitinib (Rux) treated mice corneas. Epithelial defect is presented as the percentage of the original wound size (Students  $t$ -test,  $n = 5$ ). Data are represented as mean  $\pm$  SE ( $*P < 0.05$ ,  $***P < 0.001$ ). (E) Representative immunofluorescence staining of Ki67 in control, IFN $\beta$  antibody, and Rux treated corneas at d1 post-injury. Scale bars, 200  $\mu$ m. (F) Quantifications of Ki67 positive cells from independent samples;  $n = 5$ . Data are represented as mean  $\pm$  SE ( $*P < 0.05$ ,  $**P < 0.01$ ). (G) Representative H&E images of control, IFN $\beta$  antibody, and Rux treated corneas at d7 post-injury. Scale bar, 100  $\mu$ m.

decrease in epithelial cell proliferation when IFN $\beta$  was interrupted in the wounded corneas (see Figs. 3E, 3F, Supplementary Fig. S2C). In addition, the interruption of IFN $\beta$  produced a recovered cornea with a thinner epithelium at

d7, recapitulating the RNase III phenotype observed above (see Fig. 3G). Taken together, these results suggest that IFN $\beta$  signaling is induced by dsRNA during corneal wound healing.

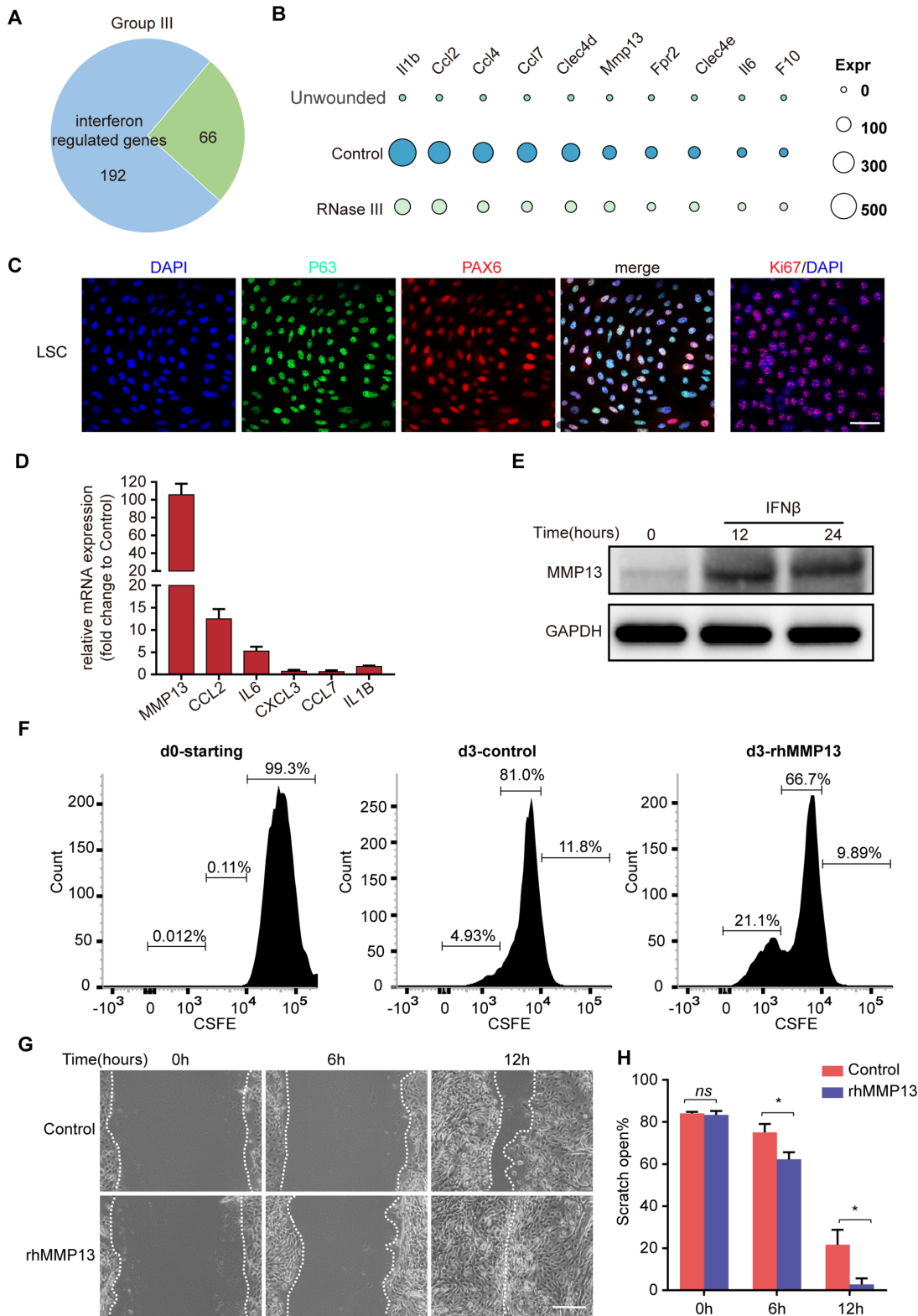


**FIGURE 4. MMP13 promotes LSCs proliferation and migration.** (A) Pie chart showing 192 genes of group III are annotated as interferon regulated genes. (B) Top 10 interferon regulated genes preferentially upregulate in wounded cornea. The size of the dot represents the gene expression. (C) Representative immunofluorescence staining of P63, PAX6, and Ki67 expression in LSCs. Scale bar, 50  $\mu$ m. (D) The qPCR analysis of top 10 genes expression in recombinant IFN $\beta$  treated LSCs ( $n = 3$ ). Data are represented as mean  $\pm$  SE. (E) Western blot analysis of MMP13 expression in recombinant IFN $\beta$  treated LSCs at indicated time points. (F) FACS analysis of carboxyfluorescein succinimidyl ester (CFSE) labeled LSCs. The original fluorescence intensity at d0 represents the starting point. The control group and recombinant MMP13 treated group are analyzed at d3. Representative data from three independent experiments are shown. (G) Scratch wound assays of control LSCs and recombinant MMP13 treated LSCs. Representative images of LSCs at indicated time-points. Scale bar, 500  $\mu$ m. (H) Quantifications of wound closure of LSCs are shown (Students  $t$ -test,  $n = 3$ ). Data are represented as mean  $\pm$  SE (\* $P < 0.05$ ).



### IFN $\beta$ Downstream Effector MMP13 Promotes LSC Proliferation

We next determined the downstream IFN $\beta$  signaling partners associated with these phenotypes. Remarkably, of the 258 genes in group III known to be downregulated by RNase III treatment, 192 were identified as interferon-responsive genes by Interferome version 2.0 (Fig. 4A). The top 10 differentially expressed genes, including inflammatory cytokines and chemokines, were selected for further validation in human LSCs (see Fig. 4B). Cultured LSCs were shown to be positive for P63, PAX6, and the cell proliferation marker Ki67 (see Fig. 4C). As expected, treatment with recombinant IFN $\beta$  upregulated the expression levels of CCL2, IL6, and IL1B (>2-fold) in these LSCs (see Fig. 4C) and matrix metalloproteinase 13 (MMP13) was significantly increased at both the mRNA (>100-fold) and protein level in response to IFN $\beta$  (see Figs. 4D, 4E). Moreover, FACS analysis showed that the lower 5,6-carboxyfluorescein diaceta succinimidyl ester

(CFSE) fluorescence intensity of rhMMP13-treated LSCs was 21.1% at d3, whereas that of control LSCs was 4.93%. Thus, recombinant MMP13 was able to accelerate LSC proliferation (see Fig. 4F). Time-point imaging assay of LSC migration showed that the rhMMP13 treated cells could completely close a scratch defect within 12 hours, whereas the scratch remained open in the control group (see Fig. 4G). Quantification of the scratch assay also confirmed the significant acceleration in scratch closure associated with the treatment of rhMMP13 in LSCs (see Fig. 4H). These findings suggest that MMP13, an interferon-stimulated gene, promotes the proliferation and migration of LSCs in vitro.

### IFN $\beta$ -MMP13 Promotes Corneal Wound Healing

This effect was further evaluated in our mouse model, where we found that *Mmp13* mRNA expression was dramatically elevated in wounded corneas when compared to unwounded controls (Fig. 5A). Immunostaining for MMP13

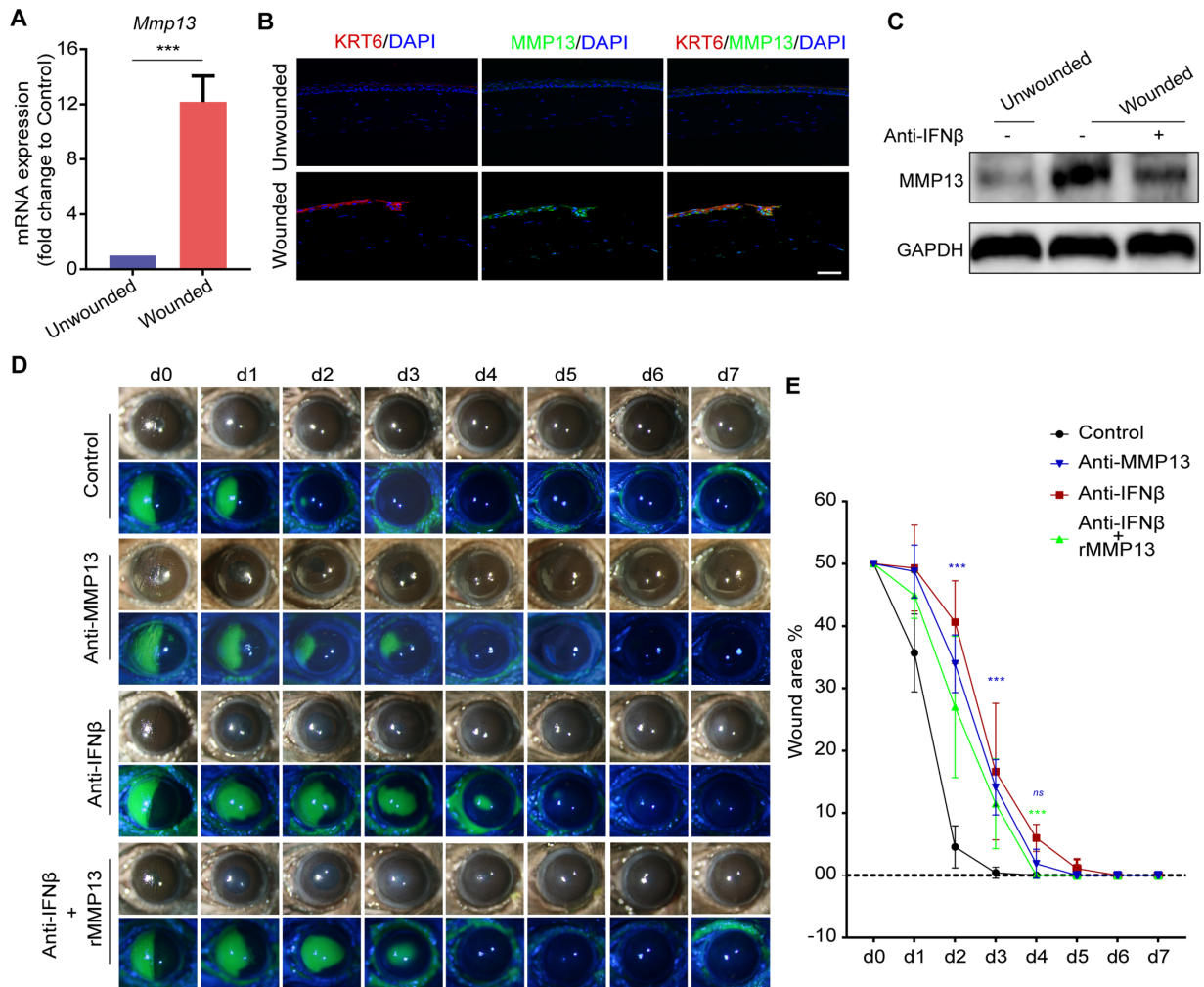


**FIGURE 5. MMP13 enhances corneal wound closure.** (A) The qPCR analysis of *Mmp13* in unwounded and wounded cornea at d1 post-injury. (B) Representative immunofluorescence staining of MMP13 and KRT6 in unwounded and wounded cornea at d1 post-injury. Scale bar, 100  $\mu$ m. (C) Western blot analysis of MMP13 proteins in unwounded cornea and wounded cornea treated with or without IFN $\beta$  antibody. Representative immunoblots are presented,  $n = 3$ . (D) Representative images of the epithelial defect in wounded corneas of control, MMP13 antibody, IFN $\beta$  antibody and IFN $\beta$  antibody combined with recombinant MMP13 treatment (for each treatment: upper panel, white light micrograph; lower panel, fluorescein staining of corneal surface). (E) Quantification of re-epithelialization in control, MMP13 antibody, IFN $\beta$  antibody, and IFN $\beta$  antibody combined with recombinant MMP13 treated mice corneas. Epithelial defect is presented as the percentage of the original wound size (Students *t*-test,  $n = 5$ ). Data are represented as mean  $\pm$  SE (\* $P < 0.05$ , \*\* $P < 0.01$ , \*\*\* $P < 0.001$ ).

also revealed that MMP13 and KRT6 were positively expressed in the corneal epithelium at d1 post wounding but were not detected in the unwounded corneas (see Fig. 5B). Meanwhile, this wound-induced upregulation of MMP13 was attenuated following treatment with an IFN $\beta$  antibody (see Fig. 5C). As expected, injured corneas treated with an MMP13 antibody were still not closed on d3 post wounding (wound area:  $14.1 \pm 2.0\%$ ) when compared with the control group. Taken together, these data suggests that MMP13 plays a key role in corneal wound healing (see Figs. 5D, 5E). Moreover, delayed wound healing caused by the neutralization of IFN $\beta$  could be rescued by the administration of rMMP13. By d4, full recovery of the corneal surface was observed in both the IFN $\beta$  antibody and rMMP13 treated group, whereas the wound area remained  $4.6\% \pm 0.8\%$  open in the IFN $\beta$  antibody-treated group (see Figs. 5D, 5E). These results confirmed that MMP13 acts as a downstream effector of IFN $\beta$  to facilitate corneal wound repair *in vivo*.

## DISCUSSION

Our study shows that a novel IFN $\beta$ -MMP13 axis is essential for corneal wound healing. Based on our findings, we propose that the following events occur during corneal injury and repair: (1) dsRNA is released from the damaged cells upon injury, (2) this dsRNA triggers IFN $\beta$  expression in the corneal epithelium, and (3) MMP13 acts as a downstream effector of IFN $\beta$  and promotes corneal epithelial cell proliferation and migration (Fig. 6).

Several lines of evidence support the idea that dsRNA released by dying or damaged cells are an early molecular signal initiating tissue regeneration.<sup>16,19</sup> Although we could not entirely eliminate dsRNA during our corneal wound healing process, our data does show that dsRNA plays a key role in corneal recovery after injury. Interruption of dsRNA resulted in a significant delay in wound closure and impaired reconstruction of the corneal epithelium during the 7-day healing process. Moreover, GO analysis revealed that the regulation of collagenic metabolic processes was disrupted following RNase III treatment in injured corneas, and induced disarranged collagen fibers in the corneal stroma following wound closure. It is possible that this impaired matrix may be related to the delayed healing of the epithelial wound evaluated in this study. However, wound closure does not indicate the completion of corneal regeneration, which may take months. Thus, the long-term effect of dsRNA on corneal injury still requires further investigation.

Interferons were originally identified as antiviral cytokines during viral infection and are known to regulate both the adaptive and innate antiviral immune responses.<sup>20–23</sup> Local administration of IFN $\alpha$ , which successfully reduces HPV load in infected cells, has been used to treat conjunctival papillomatosis.<sup>24</sup> In eye diseases, ocular surface autoimmunity is mediated by Th17 cells via IL-17A and IFN $\gamma$ .<sup>25</sup> IFN $\beta$  production of epidermis also plays a vital role in skin wound healing.<sup>21,26,27</sup> Locally injected recombinant IFN $\beta$  on the palatal mucoperiosteal wound stimulated re-epithelialization.<sup>28</sup> Here, we found that IFN $\beta$  was specifically induced by dsRNA in the corneal epithelium upon injury and mediated corneal wound closure. Of note, TLR3 has been shown to be a mediator that can recognize dsRNA and induce IFNs production.<sup>29,30</sup> Thus, it will be interesting to explore whether the dsRNA TLR3 IFN $\beta$  signal is involved in the corneal wound healing process.

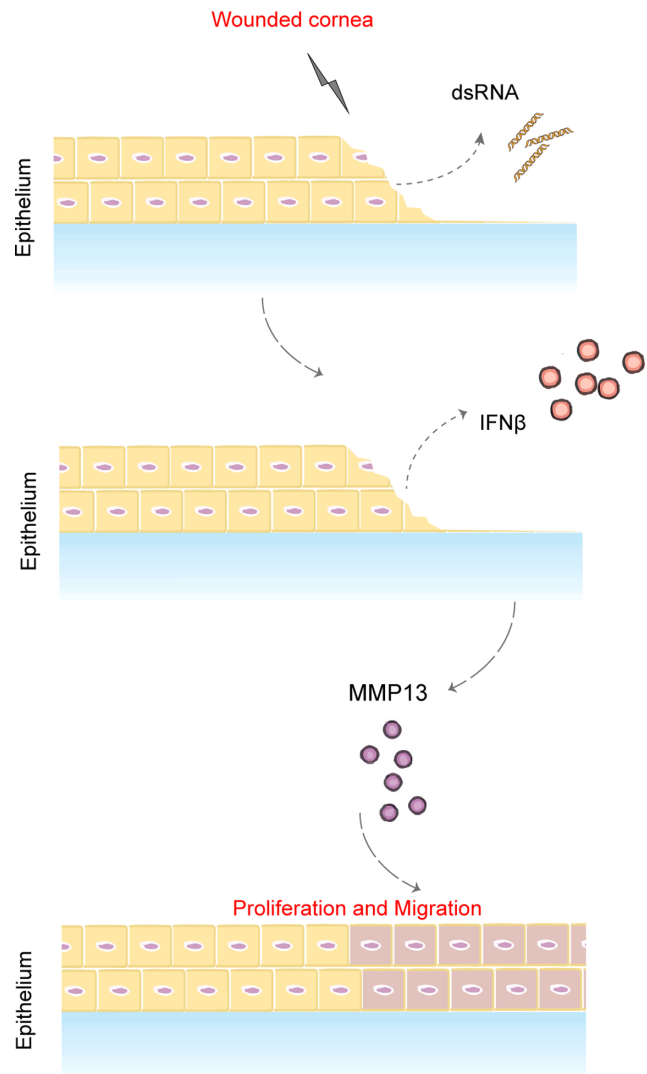


**FIGURE 6. Corneal wound healing process.** (1) The dsRNA is released from damaged cells in wounded cornea, (2) the dsRNA triggers IFN $\beta$  expression in corneal epithelium, and (3) MMP13 exerts as a downstream effector of IFN $\beta$  and promotes corneal epithelial cells proliferation and migration.

MMP13 was identified as a downstream effector of IFN $\beta$  that could enhance corneal wound repair. Notably, hundreds of ISGs, including inflammatory cytokines, were shown to be upregulated in the wounded corneas evaluated in this study, with many of these ISGs having been shown to be involved in numerous pathological and homeostatic processes, including regulation of cell proliferation, survival, migration, and protein degradation.<sup>31</sup> Upregulation of IL-6 in the early stages of keratitis could recruit polymorphonuclear neutrophils to defend against infectious pathogens.<sup>32</sup> Whereas proinflammatory cytokine IL1B modulates the corneal wound healing process via p16-STAT3 signaling.<sup>33</sup> In addition, CCL2 and its primary receptor CCR2 are associated with macrophage infiltration and neovascularization following corneal injury.<sup>34</sup> Further studies are needed to investigate the function of the other ISGs in the corneal wound healing process.

Corneal injury may result in susceptibility scarring, opacification, and loss of visual acuity.<sup>6,35</sup> Proper wound repair

is vital for corneal epithelial integrity and transparency.<sup>36,37</sup> Our work provides new insights into the corneal wound healing process and identifies the IFN $\beta$ -MMP13 axis as a potential therapeutic target to promote corneal regeneration.

### Acknowledgments

Supported by Projects of International Cooperation and Exchanges NSFC (No. 32061160364), National Natural Science Foundation of China (No. 81721003), Guangdong Basic and Applied Basic Research Foundation (No. 2021A1515012076), and Guangdong Innovative and Entrepreneurial Research Team Program (No. 2016ZT06S029).

Disclosure: **X. Lan**, None; **W. Zhang**, None; **J. Zhu**, None; **H. Huang**, None; **K. Mo**, None; **H. Guo**, None; **L. Zhu**, None; **J. Liu**, None; **M. Li**, None; **L. Wang**, None; **C. Liu**, None; **J. Ji**, None; **H. Ouyang**, None

### References

- Ouyang H, Xue Y, Lin Y, et al. WNT7A and PAX6 define corneal epithelium homeostasis and pathogenesis. *Nature*. 2014;511:358–361.
- Bashir H, Seykora JT, Lee V. Invisible Shield: Review of the Corneal Epithelium as a Barrier to UV Radiation, Pathogens, and Other Environmental Stimuli. *J Ophthalmic Vis Res*. 2017;12:305–311.
- Pellegrini G, Golisano O, Paterna P, et al. Location and clonal analysis of stem cells and their differentiated progeny in the human ocular surface. *J Cell Biol*. 1999;145:769–782.
- Davanger M, Evensen A. Role of the pericorneal papillary structure in renewal of corneal epithelium. *Nature*. 1971;229:560–561.
- Saghizadeh M, Kramerov AA, Svendsen CN, Ljubimov AV. Concise Review: Stem Cells for Corneal Wound Healing. *Stem Cells*. 2017;35:2105–2114.
- Bukowiecki A, Hos D, Cursiefen C, Eming SA. Wound-Healing Studies in Cornea and Skin: Parallels, Differences and Opportunities. *Int J Mol Sci*. 2017;18:1257.
- Foulsham W, Coco G, Amouzegar A, Chauhan SK, Dana R. When Clarity Is Crucial: Regulating Ocular Surface Immunity. *Trends Immunol*. 2018;39:288–301.
- Ljubimov AV, Saghizadeh M. Progress in corneal wound healing. *Prog Retin Eye Res*. 2015;49:17–45.
- Zieske JD, Takahashi H, Hutcheon AE, Dalbone AC. Activation of epidermal growth factor receptor during corneal epithelial migration. *Invest Ophthalmol Vis Sci*. 2000;41:1346–1355.
- Lu L, Reinach PS, Kao WW. Corneal epithelial wound healing. *Exp Biol Med (Maywood)*. 2001;226:653–664.
- Nakamura Y, Sotozono C, Kinoshita S. The epidermal growth factor receptor (EGFR): role in corneal wound healing and homeostasis. *Exp Eye Res*. 2001;72:511–517.
- Nagano T, Nakamura M, Nakata K, et al. Effects of substance P and IGF-1 in corneal epithelial barrier function and wound healing in a rat model of neurotrophic keratopathy. *Invest Ophthalmol Vis Sci*. 2003;44:3810–3815.
- Arranz-Valsero I, Soriano-Romani L, Garcia-Posadas L, Lopez-Garcia A, Diebold Y. IL-6 as a corneal wound healing mediator in an in vitro scratch assay. *Exp Eye Res*. 2014;125:183–192.
- Lai Y, Di Nardo A, Nakatsuji T, et al. Commensal bacteria regulate Toll-like receptor 3-dependent inflammation after skin injury. *Nat Med*. 2009;15:1377–1382.
- Kono H, Rock KL. How dying cells alert the immune system to danger. *Nat Rev Immunol*. 2008;8:279–289.
- Nelson AM, Reddy SK, Ratliff TS, et al. dsRNA Released by Tissue Damage Activates TLR3 to Drive Skin Regeneration. *Cell Stem Cell*. 2015;17:139–151.
- Ramnath D, Powell EE, Scholz GM, Sweet MJ. The toll-like receptor 3 pathway in homeostasis, responses to injury and wound repair. *Semin Cell Dev Biol*. 2017;61:22–30.
- Sweet M, Mansell A. The nicer side of innate immunity: Wound healing and tissue regeneration. *Semin Cell Dev Biol*. 2017;61:1–2.
- Lin Q, Wang L, Lin Y, et al. Toll-like receptor 3 ligand polyinosinic:polycytidylic acid promotes wound healing in human and murine skin. *J Invest Dermatol*. 2012;132:2085–2092.
- Muller U, Steinhoff U, Reis LF, et al. Functional role of type I and type II interferons in antiviral defense. *Science*. 1994;264:1918–1921.
- Zhang LJ, Sen GL, Ward NL, et al. Antimicrobial Peptide LL37 and MAVS Signaling Drive Interferon-beta Production by Epidermal Keratinocytes during Skin Injury. *Immunity*. 2016;45:119–130.
- Sun L, Miyoshi H, Origanti S, et al. Type I interferons link viral infection to enhanced epithelial turnover and repair. *Cell Host Microbe*. 2015;17:85–97.
- Wang Y, Yuan S, Jia X, et al. Mitochondria-localised ZNF1 functions as a dsRNA sensor to initiate antiviral responses through MAVS. *Nat Cell Biol*. 2019;21:1346–1356.
- Kaliki S, Singh S, Iram S, Tripuraneni D. Recombinant interferon alpha 2b for ocular surface squamous neoplasia: An efficient and cost-effective treatment modality in Asian Indian patients. *Indian J Ophthalmol*. 2016;64:702–709.
- Chen Y, Chauhan SK, Shao C, Omoto M, Inomata T, Dana R. IFN-gamma-Expressing Th17 Cells Are Required for Development of Severe Ocular Surface Autoimmunity. *J Immunol*. 2017;199:1163–1169.
- Di Domizio J, Belkhdja C, Chenuet P, et al. The commensal skin microbiota triggers type I IFN-dependent innate repair responses in injured skin. *Nat Immunol*. 2020;21:1034–1045.
- Bhartiya D, Sklarsh JW, Maheshwari RK. Enhanced wound healing in animal models by interferon and an interferon inducer. *J Cell Physiol*. 1992;150:312–319.
- Cornelissen AM, Von den Hoff JW, Maltha JC, Kuijpers-Jagtman AM. Effects of locally injected interferon-beta on palatal mucoperiosteal wound healing. *J Oral Pathol Med*. 2002;31:518–525.
- Pandey S, Kawai T, Akira S. Microbial sensing by Toll-like receptors and intracellular nucleic acid sensors. *Cold Spring Harb Perspect Biol*. 2014;7:a016246.
- Lewandowska-Polak A, Brauncajs M, Jarzebska M, et al. Toll-Like Receptor Agonists Modulate Wound Regeneration in Airway Epithelial Cells. *Int J Mol Sci*. 2018;19:2456.
- de Veer MJ, Holko M, Frevel M, et al. Functional classification of interferon-stimulated genes identified using microarrays. *J Leukoc Biol*. 2001;69:912–920.
- Cole N, Krockenberger M, Bao S, Beagley KW, Husband AJ, Willcox M. Effects of exogenous interleukin-6 during *Pseudomonas aeruginosa* corneal infection. *Infect Immun*. 2001;69:4116–4119.
- Wang X, Zhang S, Dong M, Li Y, Zhou Q, Yang L. The proinflammatory cytokines IL-1 $\beta$  and TNF- $\alpha$  modulate corneal epithelial wound healing through p16(Ink4a) suppressing STAT3 activity. *J Cell Physiol*. 2020;235:10081–10093.



34. Wolf M, Clay SM, Zheng S, Pan P, Chan MF. MMP12 Inhibits Corneal Neovascularization and Inflammation through Regulation of CCL2. *Sci Rep.* 2019;9:11579.
35. Hu X, Zhu S, Liu R, et al. Sirt6 deficiency impairs corneal epithelial wound healing. *Aging (Albany NY).* 2018;10:1932–1946.
36. Loureiro RR, Gomes JAP. Biological modulation of corneal epithelial wound healing. *Arq Bras Oftalmol.* 2019;82:78–84.
37. Li M, Huang H, Li L, et al. Core transcription regulatory circuitry orchestrates corneal epithelial homeostasis. *Nat Commun.* 2021;12:420.